

Muon spin rotation study of the $(TMTSF)_2ClO_4$ system

A.J. Greer^a, D.R. Harshman^{bc}, W.J. Kossler^d, A. Goonewardene^d, D.Ll. Williams^e, E. Koster^e, W. Kang^f, R.N. Kleiman^g, and R.C. Haddon^h

^aPhysics Department, Gonzaga University, Spokane, WA 99258-0051, USA

^bPhysikon Research Corporation, PO Box 1014, Lynden, WA 98264-1014, USA

^cDepartment of Physics, University of Notre Dame, Notre Dame, IN 46556, USA

^dPhysics Department, College of William and Mary, Williamsburg, VA 23187-8795, USA

^eDepartment of Physics, University of British Columbia, Vancouver, BC V6T 1Z1, Canada

^fDepartment of Physics, University of Chicago, Chicago, IL 60637, USA

^gLucent Technologies, Bell Labs, Murray Hill, NJ 07974, USA

^hDepartment of Chemistry, University of California at Riverside, Riverside, CA 92521, USA

We report a study of the organic compound $(TMTSF)_2ClO_4$ in both a sample cooled very slowly through the anion ordering temperature (*relaxed* state) and a sample cooled more rapidly (*intermediate* state). For the *relaxed* state the entire sample is observed to be superconducting below about $T_c \simeq 1.2$ K. The second moment of the internal field distribution was measured for the relaxed state yielding an in-plane penetration depth of $\simeq 12000$ Å. The *intermediate* state sample entered a mixed phase state, characterized by coexisting macroscopic sized regions of superconducting and spin density wave (SDW) regions, below $T_c \simeq 0.87$ K. These data were analyzed using a back-to-back cutoff exponential function, allowing the extraction of the first three moments of the magnetic field distribution. Formation of a vortex lattice is observed below 0.87 K as evidenced by the diamagnetic shift for the two fields in which we took *intermediate* state data.

Key words: organic superconductor, penetration depth, gap symmetry, spin density wave

Introduction

The organic superconductors $(TMTSF)_2X$ (Bechgaard salts, where $TMTSF$ means tetramethyltetraselenafulvalene), and where X is PF_6 , ClO_4 , etc., have been under much scrutiny of late due to their rich array of magnetic behavior[1,2,3,4,5]. The PF_6 compound undergoes a metal-insulator transition at ambient pressure and below 12 K enters a spin density wave (SDW) state. Under relatively low pressure, this material goes into a superconducting state with $T_c \simeq 1.1$ K[6,7]. The ClO_4 compound, however, becomes superconducting at ambient pressure if it is cooled slowly enough through the anion (ClO_4) order-

ing temperature, $\simeq 24$ K[8]. The slow cooling through the ordering temperature allows the anions to become ordered, and this is termed the *relaxed state* of the material. If, in contrast, the ClO_4 compound is cooled rapidly through the ordering temperature it enters a SDW phase below about 4 K. Between these two extremes are a whole series of *intermediate states*. These are achieved by first slowly cooling the sample from about 40 K down to a quenching temperature, and then quenching the sample by rapidly cooling to liquid helium temperatures at a rate of at least 60 K/min. When the quenching temperature is varied around the anion ordering temperature of 24 K[6], a partial degree of anion order results. Samples treated in this manner have been observed to have coexisting, macroscopically sized regions of both superconducting and SDW

phases[9].

Recently there has been much investigation into the superconducting state of these materials. As with the high- T_c 's, much of the interest has focused on the nature of the pairing state of the superconducting quasi-particles. In the early 80's there was evidence in favor of both conventional BCS-like pairing[1,10,11,12] as well as p -wave pairing[13,14,15,16]. More recently there has been much evidence from upper critical field measurements[17,18], Knight shift measurements [19,20], and corresponding theoretical support[21,22,23,24] suggesting that the pairing state may be triplet, or f -wave, in nature.

Reported here are the results of one of the few studies employing μ SR to investigate this material. We present results of *relaxed* ClO_4 in a transverse magnetic field of 300 Oe. Also presented are results of an *intermediate* state at two different transverse magnetic fields, 100 Oe and 190 Oe.

Experiment

All samples were made by the usual electrochemical technique[6]. The first sample consisted of long needles of typical dimensions 2 cm \times 2 mm \times 0.5 mm along the **a**, **b**, and **c** directions, respectively, and was studied in the *relaxed* state. The second was assembled from pieces of typical dimensions 5 mm \times 1 mm \times 0.5 mm and was studied in the *intermediate* state. For both samples, the crystals were oriented into a mosaic with axes parallel.

The data were acquired at the M15 muon beam line at the TRIUMF cyclotron facility in Vancouver, BC, Canada. The samples were mounted on 99.999% pure annealed silver (in which muons do not depolarize) and cooled in a dilution refrigerator. The *relaxed* state sample was first cooled from 80 \rightarrow 32 K at a rate of 267 mK/min and then from 32 \rightarrow 15 K at a rate of 30 mK/min. The *intermediate* state sample was cooled at a rate of 50 mK/min from 30 \rightarrow 16 K through the anion ordering temperature. Cooling was again done in zero external field.

All data were acquired with the external field applied parallel to the crystal **c** axis. The initial muon polarization direction was approximately

perpendicular to the applied field in a standard transverse field geometry. For a more complete discussion of the μ SR technique, see, *e.g.*, [25].

Results for the *relaxed* state sample

The analysis of the *relaxed* data was performed using the following Gaussian relaxation function:

$$G(t) = Ae^{-\sigma^2 t^2} \cos(\omega t + \phi) \quad (1)$$

We have omitted the 1/2 factor in the exponent for simplicity, and we used a single component function because the large sample size prevented any appreciable background in the data. The results of fits with this function are shown in Fig. 1.

The superconducting transition is clearly evident at about 1.1 K, where the formation of a flux lattice develops. This is consistent with previously published values for T_c [6,7]. The increase in the relaxation rate σ with decreasing temperature indicates a broadening of the field distribution due to the formation of a flux line lattice (FLL) in the superconducting state. The shape of this plot can often yield information on the pairing state of the superconducting quasiparticles[26]. The curve through the data is a guide to the eye using the two-fluid model for the temperature dependence of the penetration depth. That is [27]:

$$\langle(\Delta B)^2\rangle = \frac{2\sigma^2}{\gamma_\mu^2} = \frac{0.00371\phi_o^2}{\lambda^4(T)} \quad (2)$$

and with

$$\lambda(T) = \lambda(T=0) \left[1 - \left(\frac{T}{T_c} \right)^4 \right]^{-1/2} \quad (3)$$

Here, $\phi_o = 2.068 \times 10^{-7}$ G cm² is the flux quantum, $\langle(\Delta B)^2\rangle$ is the second moment, and $\gamma_\mu = 85.137$ Mrad/s/kG is the muon gyromagnetic ratio. For equation 2 a triangular lattice is assumed, and the value for σ is found from Fig. 1 by subtracting the above T_c value from the $T \rightarrow 0$ K value in quadrature. The low temperature penetration depth for these data was previously determined to be $\lambda_{ab} = 12000 \pm 2000$ Å[7], where λ_{ab} is an average penetration depth obtained from equation 2. Since the penetration depths along **a**

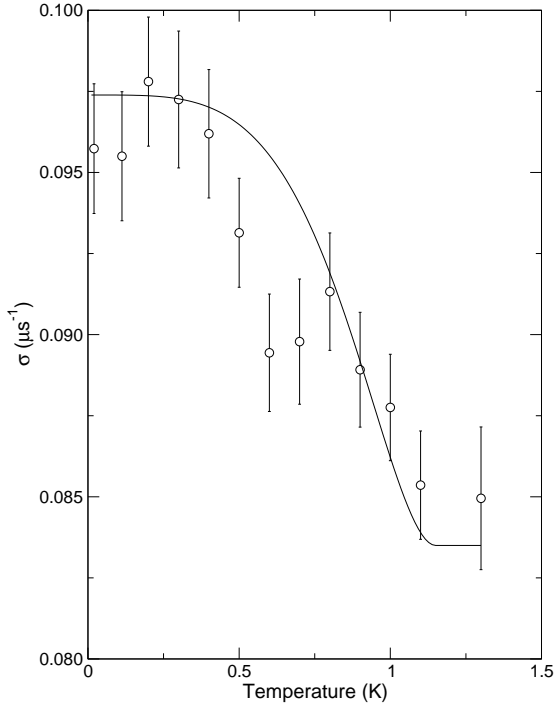


Figure 1. Plot of the relaxation rate σ as a function of temperature for the *relaxed* (superconducting) state at $H_{ext} = 300$ Oe. The curve is a fit using the two-fluid model assuming a baseline of $0.0835 \mu\text{s}^{-1}$ and $T_c = 1.15$ K, yielding $\lambda(T \rightarrow 0 \text{ K}) = 12300 \text{ \AA}$.

and \mathbf{b} are different this $\lambda_{ab} = \sqrt{\lambda_a \lambda_b}$. Field distributions expected when $\lambda_a \neq \lambda_b$ can be seen in ref[28]. Our data appear to become temperature independent as 0 K is approached, which is consistent with *s*-wave pairing; however, it is not possible to precisely determine the pairing state due to the size of the error bars.

The data here, in contrast to those of L.P. Le *et al.*[29], have many more low temperature points. The clear rise in relaxation rate, seen in our data below about 1 K, may have even been seen in their data, but was discounted due presumably to the sparseness and lower statistics of their data.

Results for the sample in the *intermediate* state

Before taking data and lowering the sample temperature, an external field of 100 Oe was applied and held fixed during this phase of the experiment. The analysis was performed using a back-to-back exponential function of the form[30]

$$n(\omega) = \begin{cases} a_L e^{(\omega - \omega_p)\tau_L} & (\omega < \omega_p) \\ a_R e^{(\omega_p - \omega)\tau_R} & (\omega > \omega_p) \end{cases} \quad (4)$$

to represent the fields associated with superconductivity. Here ω_p is the frequency of the peak of the frequency distribution, ω is the frequency, τ_L and τ_R are the decay factors to the left and right of the peak frequency, a_L and a_R are constants, and $n(\omega)$ is the probability per unit frequency interval of a given frequency. An assumed Gaussian-like distribution of fields arising from nuclear dipoles was convoluted with this. This convoluted form has an analytical Fourier transform which was used as the first component of a two component fitting function. The second (*background*) component is attributed to muons which do not stop in the sample. This sample was of a smaller size than the *relaxed* sample, and we found it appropriate to include a background signal. The overall fitting function is shown below.

$$G(t) = A_1 B(t) e^{-(\sigma_1 t)^2} + A_2 e^{-(\sigma_2 t)^2} \cos(\omega_2 t + \phi) \quad (5)$$

Subscripts here refer to first and second components. Also,

$$B(t) = (r_1(t) + r_2(t)) \cos(\omega_1 t + \phi) + t(r_1(t)/\tau_L - r_2(t)/\tau_R) \sin(\omega_1 t + \phi) \quad (6)$$

and

$$r_1(t) = \frac{\tau_R}{(\tau_L + \tau_R)(1 + (t/\tau_L)^2)} \\ r_2(t) = \frac{\tau_L}{(\tau_L + \tau_R)(1 + (t/\tau_R)^2)} \quad (7)$$

The nuclear dipole field spread parameter, σ_1 , and the *background* parameters (A_2 , σ_2 , and ω_2) were determined by fits above T_c and were held fixed for subsequent fits. (For the 190 Oe data these parameters were found *at* T_c due to the behavior above T_c – see below.) The parameters in

$B(t)$ then reflect *changes* in the magnetic environment seen by the muons.

Results of fits are expressed as moments of the field distribution. First, second, and third moments for the applied field of 100 Oe are shown in Fig. 2 as diamonds. The onset of superconductiv-

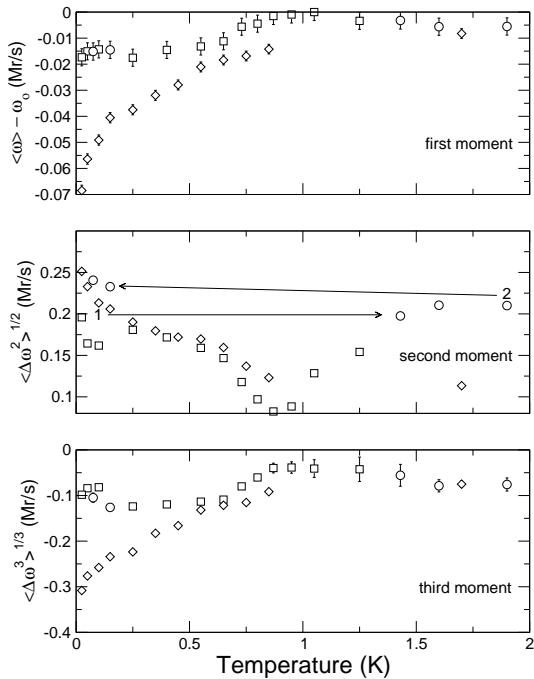


Figure 2. Plot of the first, second, and third moments of the field distributions derived from the back to back exponential function fits: 100 Oe applied field (diamonds), 190 Oe applied field (circles, squares).

ity is at $T_c \simeq 0.87$ K, a little lower than the *relaxed* state discussed above, and consistent with earlier studies of *intermediate* state samples[9]. One can see immediately from the second moment data that the behavior as $T \rightarrow 0$ K is different than the *relaxed* sample data as well as what conventional BCS theory predicts. The increasing second mo-

ment denotes very unusual behavior, which we attribute to the mixed phase state of the sample.

The first and third moment graphs show increases in diamagnetic shift and skewness, respectively, as $T \rightarrow 0$ K. Contrary to expectations, the skew is toward lower fields. This lower field skewness may be, for example, seen directly in Fig. 3. The tail to the left of the peak is responsible for the skewness. The lower field tail is not

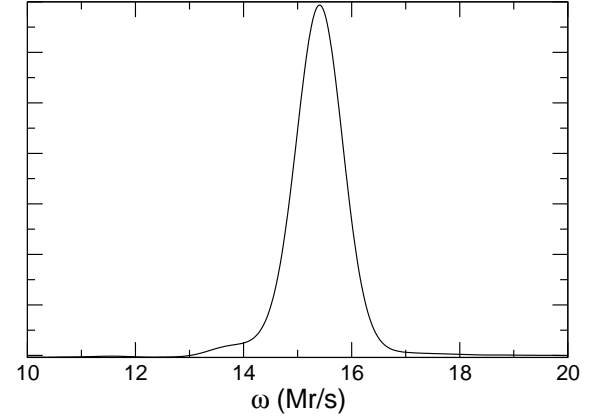


Figure 3. The lineshape at $T = 0.025$ K for 190 Oe showing the low field tail giving the negative third moment.

predicted for either a triangular or square flux lattice alone[27], and is most likely due to the SDW phase.

The results of fits to data with $H_{ext} = 190$ Oe applied parallel to the crystal \mathbf{c} axis are also shown in Fig. 2. The second moment graph (circles and squares) again clearly shows the onset of superconductivity at $T_c \simeq 0.87$ K. Below this temperature the field distribution broadens as fluxons in the superconducting phase form into some type of lattice. Above T_c the fits surprisingly show evidence of a broad field distribution which increases with temperature. This must be due to the SDW phase, since the superconducting regions are not present here. As T_c is approached from above, the field distribution seen

by the muons becomes more uniform, reflecting the decreasing influence of the SDW phases in favor of the uniform, applied field. Below T_c the behavior is generally the same as for the 100 Oe data, but with more scatter at low temperature. The reason for this scatter, we think, is due to the order in which the data were taken. The square points indicate data taken while lowering the temperature monotonically from 1.25 K to 0.025 K. From 0.025 K the sample was warmed up to 1.43 K as indicated by arrow 1. The circles show results from fits as the sample was warmed to 1.90 K. Finally, the sample was cooled (more circles) to 0.15 and 0.075 K as indicated by arrow 2. These last points are higher than the previous low temperature data points for the 190 Oe field, and not much higher than the circles above T_c . We believe this final higher second moment results due to the interplay between the superconducting regions and the SDW regions.

The first and third moment graphs for 190 Oe show similar, but less dramatic, effects than for 100 Oe. In the first moment graph, the diamagnetic shift is much smaller, which may indicate that a smaller fraction of the sample is superconducting. Similarly, the third moment is less pronounced for this higher applied field. Both of these effects can be understood if one considers that the data fit by the first component of the fitting function contain signals from muons which stop in two different magnetic environments. The amount of signal from each is proportional to the number of muons stopping in each, and a higher field should decrease the superconducting fraction in favor of the SDW phase.

Conclusion

We have studied the *relaxed* and some *intermediate* states of the organic superconductor $(TMTSF)_2ClO_4$ with μ SR. While the error bars are too large to rule out higher order quasiparticle pairing, the results of fits to *relaxed* state data indicate a temperature dependence which appears to be consistent with *s*-wave pairing. The low temperature penetration depth is found to be $\lambda_{ab} = 12000 \pm 2000 \text{ \AA}$. Recent, subsequent data taken on similar samples also reveal behav-

ior consistent with *s*-wave pairing, although the authors claim otherwise[31]. The *intermediate* state, characterized by coexisting regions of superconducting and SDW phases, has a suppressed T_c and a lineshape with a low-field tail below T_c . Both of these effects are proposed to be due to the existence of this SDW phase in the material.

The authors would like to thank Mel Goode, Bassam Hitti, and the rest of the TRIUMF support personnel for their help in making this work possible.

REFERENCES

1. Stéphane Belain and Kamran Behnis, Phys. Rev. Lett. 79 (1997) 2125.
2. J.R. Cooper *et al.*, Phys. Rev. Lett. 63 (1989) 1984.
3. D. Jérôme *et al.*, J. Phys. (Paris) Lett. 56 (1980) L-95.
4. T. Osada *et al.*, Phys. Rev. Lett. 66 (1991) 1525.
5. S.T. Hannahs *et al.*, Phys. Rev. Lett. 63 (1989) 1988.
6. T. Ishiguro *et al.*, Organic Superconductors, (Springer, Berlin, 1998).
7. D.R. Harshman and A.P. Mills, Phys. Rev. B45 (1992) 10684; D.R. Harshman, R.N. Kleiman, R.C. Hadden, W.J. Kossler, T. Pfiz, and D.Ll. Williams, unpublished; D.R. Harshman, Invited talk presented at the Gordon Research Conference on Organic Superconductivity, Irsee, Germany, 22-27 September, 1991.
8. K. Bechgaard *et al.* Phys. Rev. Lett. 46 (1981) 852.
9. H. Schwenk *et al.*, Phys. Rev. B29 (1984) 500.
10. P. Garoche *et al.*, J. Physique Lett. 43 (1982).
11. P.M. Chaikin *et al.*, J. Magn. Magn. Mater. 31 (1993) 1268.
12. K. Murata *et al.*, Japn. J. Appl. Phys. 26 (1987) 1367.
13. M.Y. Choi *et al.*, Phys. Rev. B 25 (1982) 6208.
14. S. Bouffard *et al.*, J. Phys. C: Solid State Phys. 15 (1982) 2951.
15. C. Coulon *et al.*, J. Physique 43 (1982) 1721.
16. S. Tomic *et al.*, J. Physique Coll. C3 (1983) 1075.

17. I.J. Lee *et al.*, Synth. Metals 70 (1995) 747.
18. I.J. Lee *et al.*, Phys. Rev. Lett. 78 (1997) 3555.
19. I.J. Lee *et al.*, unpublished cond-mat/0001332.
20. I.J. Lee *et al.*, Phys. Rev. Lett. 88 (2002) 17004.
21. R.D. Duncan *et al.*, unpublished cond-mat/0102439.
22. A.G. Lebed *et al.*, Phys. Rev. B62 (2000) R795.
23. K. Kuroki *et al.*, Phys. Rev. B63 (2001) 094509.
24. M. Miyazaki *et al.*, unpublished cond-mat/9908488.
25. A. Schenck, Muon Spin Rotation Spectroscopy: Principles and Applications in Solid State Physics (Hilger, Bristol, 1986).
26. M. Tinkham, Introduction to Superconductivity (McGraw-Hill, New York, 1975).
27. E.H. Brandt, J. Low Temp. Phys. 73 (1988) 355.
28. A.J. Greer and W.J. Kossler, Low magnetic fields in anisotropic superconductors (Springer-Verlag, Berlin, 1995).
29. L.P. Le *et al.*, Phys. Rev. B48 (1993) 7284.
30. D.R. Harshman *et al.*, Phys. Rev. Lett. 67 (1991) 3152.
31. G.M. Luke *et al.*, to be published in Physica B.